

The Rheology of Paraffin Wax and its Usefulness as an Analogue for Rocks

NEIL S. MANCKTELOW

Mancktelow, N.S. 1988 12 30: The rheology of paraffin wax and its usefulness as an analogue for rocks. *Bulletin of the Geological Institutions of the University of Uppsala*, N.S., vol 14, pp. 181–193. Uppsala ISSN 0302-2749.

Accurate scale modelling of geological structures demands rheological similarity between the analogue material employed and rocks under natural deformation conditions. Model materials must, therefore, be carefully calibrated within the required experimental range. For a confining stress σ_3 of 0.3 bar and strain rates in the range 5×10^{-6} to $1 \times 10^{-4} \text{ s}^{-1}$, the studied paraffin waxes exhibit power-law creep behaviour over a limited but experimentally useful temperature range. The calibrated stress exponents for the three grades of wax are 2.4, 2.8, and 4.1, with the stress exponent apparently increasing with decreasing melting point for the wax. This range is similar to the experimentally determined values for common rocks and paraffin wax therefore represents an excellent analogue for rocks deforming by power-law creep.

Neil S. Mancktelow, Geologisches Institut, ETH-Zentrum, CH-8092 Zürich, Switzerland.
Received 4th May 1987; Revision received 30th September 1987.

Introduction

With few exceptions, deformational structures in rocks are too large, develop too slowly and require forces which are too great to ever allow direct experimental observation. Experiments must therefore involve some form of scale model and it is clearly the aim of such experiments to maintain similarity between the model and the original geological process as closely as possible. The extrapolation of the results to natural examples is dependent on this similarity. This will be true regardless of whether the material is kept the same but temperature and strain rate are scaled (i.e. rock mechanics experiments) or if an analogue material, as discussed here, is employed.

The theory of mechanical scale models is well established, due to its broad applicability in many fields of engineering and applied science. Excellent reviews are provided by Ramberg (1981), Kline (1965), Porter (1958), Langhaar (1951), and Hubbert (1937). Non-mechanical processes (chemical reactions, diffusion, etc.) are by necessity excluded from this dimensional scaling, and strict experimental modelling of processes involving both metamorphism and deformation is, in general, unattainable.

Ideally, we wish to maintain geometrical (the model is a reduced or enlarged geometric replica of the original), kinematic (corresponding particles are

found at corresponding points at corresponding times) and dynamic (the ratio between various kinds of mechanical forces compared kind for kind, that act on corresponding particles in the original and model, is constant) similarity (cf. Ramberg 1981). Such comprehensive and strict scaling of geological structures is not possible under normal, non-accelerated experimental conditions because the gravitational acceleration in the natural original and in the scale model are the same, i.e. the model ratio for acceleration is 1. This immediately implies a fixed (and experimentally unrealistic) constraint on the model ratios of length and time and requires that the strength of the model materials must be very low if gravitational forces are to be correctly scaled relative to surface forces (cf. Ramberg 1981, p 39–41). Solid-state creep of rocks in geological processes is so slow, however, that inertial forces are negligible and if we restrict ourselves to fairly small-scale structures (with dimensions of less than a few hundreds of metres), the effects of gravity may also be ignored. We are then free to select independent model ratios of length and time suitable for our experiments.

However, dynamic similarity of the surface forces must still be maintained for proper scaling, and, as extensively discussed by Weijermars & Schmeling (1986), this implies that the analogue and original (rock) materials must be rheologically similar. For

corresponding particles in the model and the original, the stress-strain curve must have the same shape and may differ only in the scaling of the stress axis; the scale factor for the stress axis must be the same for every set of corresponding points. During heterogeneous deformation, different particles are experiencing different strain rates at any one time. For dynamic similarity, it can be easily shown that the stress-strain rate relationship of the original and model materials may differ only in the proportionality constant (Weijermars & Schmeling 1986). Consider the general case where, for a constant, specific temperature, the steady-state flow stress in the original rock material is directly proportional to some function of the strain rate $f_o(\dot{\epsilon}_o)$, with a proportionality constant C_o . That is:

$$\sigma_o = C_o f_o(\dot{\epsilon}_o) \quad (1)$$

For dynamic similarity, the model ratio (σ_r) of the stresses due to surface forces at any pair of geometrically corresponding points of the model (m) and original (o) must be held constant, so that:

$$\begin{aligned} \sigma_r &= \sigma_m / \sigma_o \\ &= K \quad (\text{a constant}) \end{aligned}$$

therefore,

$$\sigma_m = K \sigma_o$$

which, substituting for σ_o from equation (1) above gives:

$$\sigma_m = K C_o f_o(\dot{\epsilon}_o) \quad (2)$$

i.e. if dynamic similarity is to be maintained, the mechanical equation of state relating differential flow stress to strain rate for the analogue material may differ from that of the original rock material only in the proportionality constant. This must be true for every corresponding point in the model and in the original. For the specific case of power-law creep, where the strain rate $\dot{\epsilon}$ is proportional to σ^n , the stress exponent n of the analogue material must equal that of the rock material to be modelled.

Paraffin Wax as a Modelling Material: Previous Work

The use of analogue scale models to study geological structures has a long and productive history (see the review of Summers 1933). Paraffin waxes are

one of the more commonly employed analogue materials, but their rheology has received only limited attention (Barry & Grace 1971, Cobbold 1975, Neurath & Smith 1982). In contrast, the rheologies of several other analogue materials have been extensively investigated, e.g. Plasticene (McClay 1976) and Plasticene-like materials (Weijermars 1986), and silicon or "bouncing" putty (Dixon & Summers 1986, Weijermars 1986), as well as some potentially interesting new materials (PDMS and PBDMS of Weijermars 1986). Recent modelling studies using paraffin waxes include those of Cobbold (1975) on the propagation of single layer folds, Latham (1979) on the development of folds in anisotropic materials, Neurath & Smith (1982) on the amplification rates of folds and boudins, Baumann (1986) on the initiation of ductile shear zones, and Dixon & Simpson (1987) on the intrusion of laccoliths.

Chemical and Physical Properties of Paraffin Wax

The following is a summary from the comprehensive work of Freund et al. (1982), which is itself a compilation of the surprisingly extensive literature on the chemistry and physical properties of paraffin products and their individual components.

Chemistry

Paraffinic hydrocarbons, or paraffin, are straight-chained or branched saturated organic compounds with the composition C_nH_{2n+2} . The term paraffin waxes is used for mixtures of various hydrocarbon groups, especially paraffins and cycloalkanes, that are solid at room temperature.

The various types of paraffin waxes form essentially two groups. *Macrocrystalline paraffin waxes* are mixtures which consist chiefly of saturated, normal $C_{18}-C_{30}$ hydrocarbons and smaller amounts of iso-alkanes and cycloalkanes. The molecular weight of the components varies between 250 and 450, their melting point between 40 and 60°C. Their crystals are plate- or needle-shaped. *Microcrystalline paraffin waxes* contain, in addition to normal hydrocarbons, large amounts of iso-alkanes and napthenes with long alkyl side-chains. The iso-alkanes form microcrystals and the major part of these waxes consists of $C_{40}-C_{55}$ compounds. The melting point of microcrystalline paraffin waxes varies between 60 and 90°C.

Depending on the degree of refining, one can classify paraffin waxes as technical, semi-refined

and refined grade waxes. Technical grade paraffin waxes usually contain less than 6 wt-% oil. Semi-refined paraffin waxes may contain a maximum of 3 wt-% oil, and their colour is light yellow to white. Finally, refined paraffin waxes contain 0.4–0.8 wt-% oil; they are colourless, odourless and do not contain substances detrimental to health. The chemical composition of macro-and microcrystalline paraffin waxes varies over an almost infinite range of combinations, depending upon the source of the crude petroleum and the processing technology.

Crystallography and the α - β allotropic transition

Paraffin hydrocarbons – whether individual compounds or their mixtures – are always crystalline at temperatures below their melting point or melting range. As with many crystalline substances, a further change of the crystal structure may take place in a temperature range below the melting point. These changes – termed allotropic transitions – occur at given, so-called equilibrium transition temperatures, provided that cooling is infinitely slow. Allotropic transitions are always displayed on the cooling curve by further breaks, since they are accompanied by changes in the heat content. It is an important characteristic of allotropic transitions that they represent reversible processes, i.e. they will be repeated during heating when the corresponding equilibrium temperature is reached, provided that heating is infinitely slow. If the cooling or heating rate is finite, the transitions take place at temperatures lower or higher, respectively, than the equilibrium temperature. Therefore, the transition temperature will differ when reached by cooling or by heating, the difference being a function of the rate of temperature change (see Fig. 1).

According to several authors (see Freund et al. 1982, p. 75 and following), C_{21} to C_{36} normal paraffin hydrocarbons display a well-defined allotropic transition at some degrees Celsius below their melting point. The so-called α -phase, stable below the melting point, is converted into the β -phase, and the transition is accompanied by the release of a relatively high amount of heat. At ambient temperature, normal alkanes between C_{19} and C_{29} containing an odd number of carbon atoms have an orthorhombic structure, even-numbered normal alkanes between C_{18} and C_{26} have a triclinic structure and those between C_{28} and C_{36} a monoclinic structure. At higher temperatures, the stable structures are crystal systems of higher symmetry, in particular orthorhombic and hexagonal structures. Several authors report that normal alkanes from C_{38} onwards do not exhibit transition points: the phase stable below the melting point is the β -phase. In

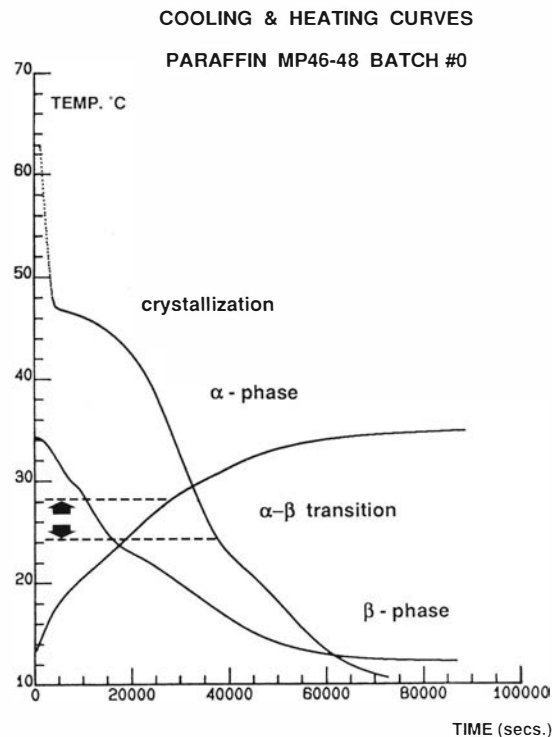


Fig. 1. Cooling and heating curves for paraffin wax of melting range 46–48°C (Batch #0). Breaks in slope correspond to phase transitions (crystallization and the α - β transition), due to the heat of transition and the differing heat capacities of the two phases. Because heating and cooling rates are not infinitely slow, the break in slope of the cooling curve always occurs below the true transition temperature and the break in the heating curve above. The curves, therefore, only allow a temperature range to be determined, within which the true transition temperature must lie.

hexagonal structures the long molecules are capable of free rotation about their longitudinal axis. Such paraffin waxes are relatively soft. In the orthorhombic crystals, free rotation of the molecules is not possible and, therefore, such paraffin waxes are more rigid.

Commercial macrocrystalline paraffin waxes consist, at ambient temperatures, mainly of hard orthorhombic crystals, but the hexagonal structure is also always present, even if only in small amounts. In addition, liquid branched hydrocarbons also participate in building up the final structure. The amount of the hexagonal form depends on the molecular mass range of the constituents. The melting range and the transition range become broader with more complex paraffin wax composition. For narrower molecular mass range fractions, the transition range is narrower. When this transition is

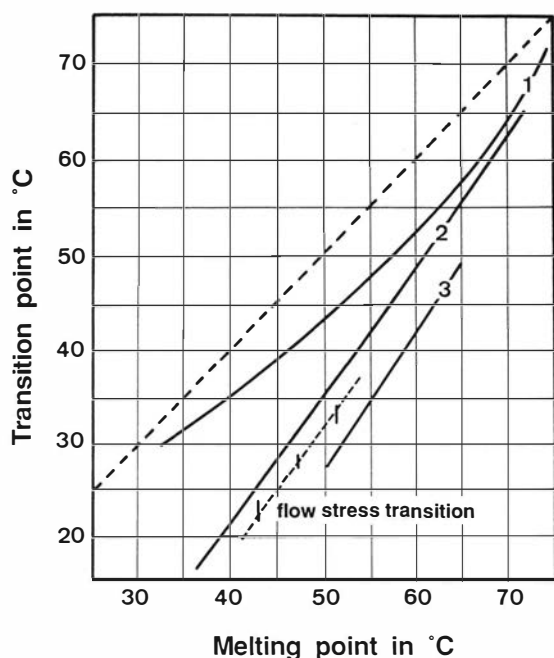


Fig. 2. Summary plot of the α - β transition temperature against melting temperature for individual n-alkanes (1), for mixtures of n-alkanes with a narrow molecular weight range (2) and for commercial paraffin waxes (3), from Freund et al. (1982). The temperature ranges within which a sudden weakening of the studied paraffin waxes occurs (the transition from field 2 to 3, see text) are also indicated. These ranges are an artifact of the temperature spacing between experiments and the actual transition may be quite sharp. An interpreted transition curve is shown dashed.

abrupt, contraction of the paraffin wax during cooling can cause cracking. The difference between the melting point and the transition range increases with the breadth of the molecular mass range of the paraffin wax.

Figure 2, modified from Freund et al. (1982), represents the transition temperatures, plotted against their melting points, of individual n-alkanes (1), n-alkane mixtures (2), and commercial paraffin waxes having different melting points (3). From curve (1), it can be seen that with increasing carbon atom numbers, i.e. with increasing melting points, the temperature difference between the transition point and the melting point decreases and finally disappears at the C₃₇ compound (i.e. for melting temperatures >76°C). Microcrystalline paraffin waxes contain C₃₃-C₆₀ n-alkanes, and hence the importance of the α - β transition is much less than in macrocrystalline paraffin waxes. From all three curves, it is obvious that, for identical melting points, the transition temperatures of commercial

paraffin waxes with broad molecular weight ranges and complex compositions (3) are lower than those for mixtures of n-alkanes (2), which in turn are lower than those of individual n-alkanes (1). The transition to markedly lower flow stresses, as determined by the deformation experiments described in detail below, which broadly corresponds with the α - β transition range as determined from heating and cooling curves (e.g. Fig. 1), are included on Fig. 2 for the analytical-grade commercial paraffin waxes investigated in the current study. It is clear that the waxes studied are highly refined, and plot in a field intermediate between the lower quality commercial waxes (curve 3) and the mixtures of n-alkanes (curve 2).

Volume change

Paraffin waxes undergo a marked contraction of around 11 vol-% on crystallizing from the melt, with an additional 3–3.5 vol-% volume reduction at the α - β transition (Freund et al. 1982, Table I-45). This results in the development of marked central depressions in moulds cast from the melt, and moulds for models must be made oversized and later machined to the correct dimensions (see below). It can also lead to internal cracking if models are cooled too rapidly from the melt and through the transition temperature.

Experimental Technique and Preparation

The three macrocrystalline paraffin waxes investigated are of analytical grade, with 2°C nominal melting ranges, and were obtained from major chemical suppliers (see Appendix). Rheological calibration was performed in the same pure shear, plane strain machine (Mancktelow 1988) and under the same conditions as used for analogue modelling experiments (e.g. Baumann 1986, Baumann & Mancktelow 1987). This has obvious advantages for interpreting the results of such experiments.

The stress-strain curve for paraffin wax has a clear elastic range, a rounded yield segment, and a flow segment which, for a specific temperature range and confining pressure, approximates a steady-state (Fig. 3). This suggests that, within this flow regime, the average internal microstructure does not change with increasing strain and simplifies calibration by allowing multiple, stepped strain rate experiments using a single block of paraffin. The paraffin is bought in 50 or 100 kg lots and arrives as a series of flat blocks. These are broken into small

Paraffin Wax Melting Point 46-48 °C

Stress (bars)

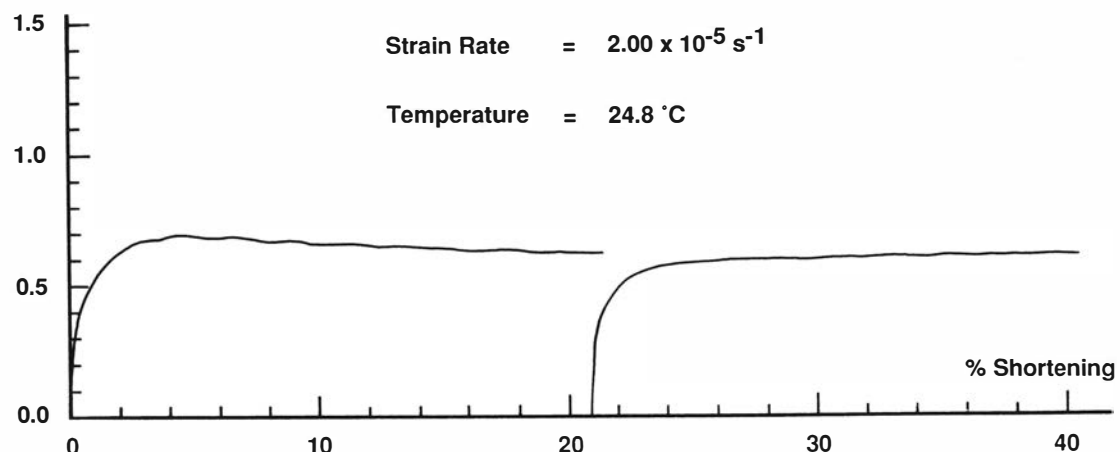


Fig. 3. Typical differential stress ($\sigma_1 - \sigma_3$) versus strain (given here as percent shortening) for paraffin wax. The excellent reproducibility is clear from the stop and restart test at around 21 % shortening.

pieces and thoroughly mixed to ensure uniformity. Unfortunately, the calibration tests have shown that differing lots from the same supplier can differ slightly but significantly in their mechanical properties (e.g. see Appendix, Batches #0 and #1 of paraffin wax MP46-48). This is an argument for buying large quantities at a time, as each new lot must be individually calibrated.

The paraffin is melted and poured into moulds which are slightly larger than the required final dimensions, to allow for uneven shrinkage on cooling. The paraffin is then cut and machined into its final shape ($29 \times 12 \times 6 \text{ cm}$) and loaded into the machine, copiously lubricated with petroleum jelly. The preset temperature is allowed to stabilize overnight (ca. 14 hours) before beginning a series of constant strain rate experiments. A constant confining stress $\sigma_3 = 0.3 \text{ bar}$ (1 bar = 10^5 pascal) was employed for all calibration experiments. Steady-state flow (if attained, see below) is well established within ca. 5–8 % shortening, allowing up to 5–6 tests within the 42 % shortening range of the machine. The strain rates are disordered within the range 5×10^{-6} to $1 \times 10^{-4} \text{ s}^{-1}$ so as to eliminate any systematic error should non-steady-state flow occur (work hardening or softening). Data collection occurs under computer control. The stress-strain curve, side stress and average strain rate are continuously displayed on a graphics terminal during the experiment and the data (strain, stress, side stress, temperature and

time) stored as a data file. After successful conclusion, the stress-strain curve is plotted and the average temperature and strain rate (least squares regression of strain against time) determined. The flow stress can then be manually read from the stress-strain curve and a data file of flow stresses for various temperatures and strain rates established.

Results

For the specific paraffin waxes and range of strain rates investigated, which adequately covers the range of current interest in our laboratory, three deformation fields have been established with increasing temperature:

- 1) a field of marked work softening, which is transitional to brittle failure at still lower temperature
- 2) a field of effectively steady-state flow
- 3) a field of flow at markedly reduced strength, the transition from field 2 to field 3 apparently corresponding to the $\alpha-\beta$ phase transition (see Fig. 2).

The calibration experiments of this study have been concentrated within field 2, where paraffin wax flows at near steady-state after yield, with only

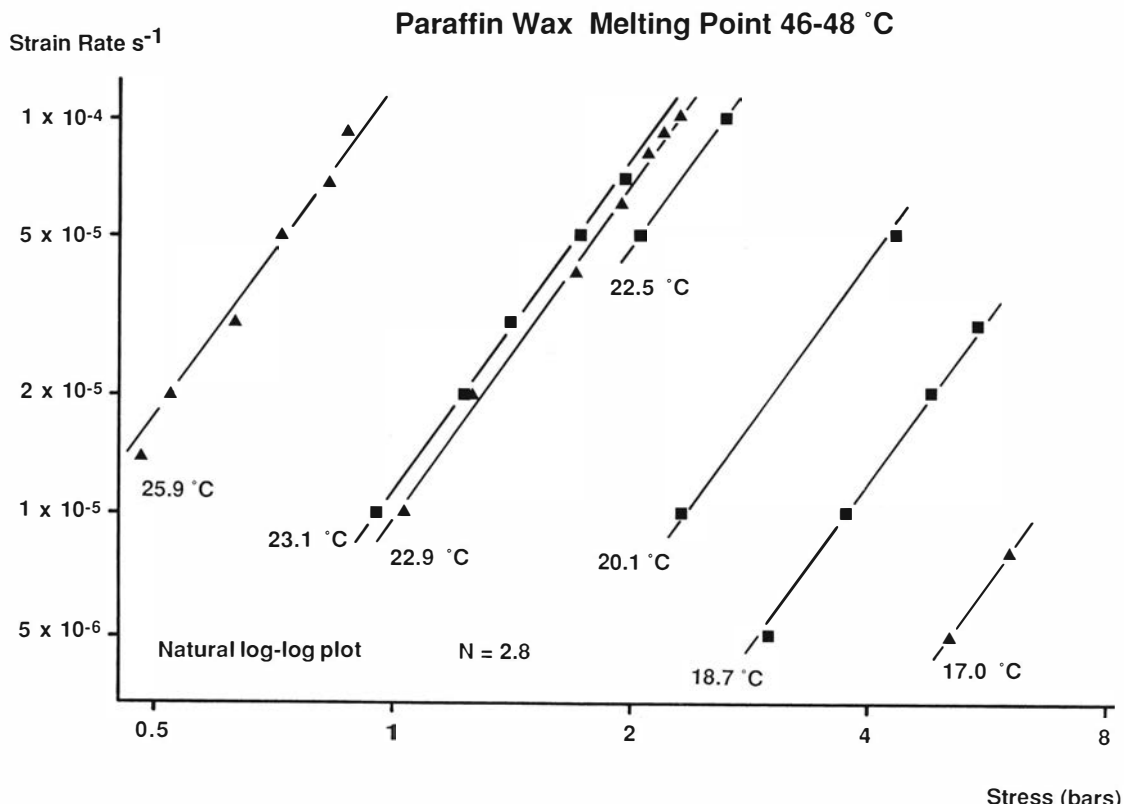


Fig. 4. $\log_e - \log_e$ plot of strain rate (s^{-1}), against stress (1 bar = 10^5 pascal for a number of constant strain rate experiments at different temperatures for paraffin wax of melting range 46–48°C (Batch #0). The log scales of the two axes are not equal; the stress axis is expanded for clarity and to give greater separation between the various experiments.

a slight tendency to work softening (Fig. 3). In this field, the phenomenological stress-strain rate behaviour of paraffin wax is accurately described by a power-law relation of the form.

$$\dot{\epsilon} = A e^{-Q/RT} \sigma^n \quad (3)$$

where $\dot{\epsilon}$ is the natural or logarithmic strain rate, A is a material constant, Q is the apparent activation energy, R is the Gas Constant, T is the temperature in °K, σ is the stress (here, given in bars), and n the stress exponent. Strictly, the stress should be normalized against the elastic shear modulus μ , to produce a dimensionless value for $(\sigma/\mu)^n$ (e.g. Poirier 1985), such that the material constant A has rational dimensions of strain rate (in our case s^{-1}). However, in common with most rock mechanics studies, the shear modulus has not been accurately measured and the stress-strain rate relationship is presented as in equation (3), with the attendant disadvantage that A has non-rational dimensions (e.g. Carter 1976, equation 5).

Taking the natural logarithm of both sides of (3) gives:

$$\ln \dot{\epsilon} = \ln A - Q/RT + n \ln \sigma$$

which has the form of a linear equation (with three variables $\ln \dot{\epsilon}$, $1/RT$, and $\ln \sigma$), allowing a standard regression of the measured data. An example of the measured data for paraffin wax with a melting point of 46–48°C is presented graphically in Fig. 4, and all data, together with the results of the regressions, are listed in the Appendix.

As can be seen from the regression results, this relation can generally predict the data values to within the experimental error ($\pm 5\%$), and is perfectly adequate for interpolation. The determined material constant A , apparent activation energy Q and stress exponent n for the calibrated paraffin waxes are summarized in Table 1. The small temperature range of the experiments is restricted by the limited extent of the steady-state power-law creep field (field 2). This in turn restricts

Table 1

Melting Range °C	$\log_e A$	Q (kcal/mol)	n
42–44	248	149	4.1
46–48 (Batch #0)	243	150	2.8
46–48 (Batch #1)	204	126	2.7
50–52	201	127	2.4

the degree of constraint on the determined activation energy Q.

Previous published work on the rheology of paraffin is rather limited, despite its common use in analogue modelling experiments. Cobbold (1975) reported power-law behaviour for two grades of paraffin wax of melting point 52°C and 54°C. The measured stress exponent of 2.6 is similar to that determined in this study for paraffin wax of similar melting point but from different suppliers. Neurath & Smith (1982) report an exponent of 1.8 for paraffin wax of unknown melting point.

For the experimental conditions of constant least compressive stress, $\sigma_3 = 0.3$ bar, the ratio of the effective confining pressure (equivalent to the mean stress $(\sigma_1 + \sigma_2 + \sigma_3)/3$) to the differential flow stress $(\sigma_1 - \sigma_3)$ will decrease with increasing flow stress, which can be produced by decreasing the temperature or increasing the strain rate. Above a certain yield stress (of around 3.5–4 bar for $\sigma_3 = 0.3$ bar), there is a clearly discernable and increasing tendency (with increasing flow stress) towards significant strain softening following yield, and true steady-state flow is not established (field 1). There is no initial through-going fracture or general lack of cohesion. Instead, close examination reveals a multitude of small conjugate "shear zones", generally < 1 cm long, which nucleate on imperfections (e.g. small air bubbles) and are made clear by the tendency for non-cohesive zones in paraffin to appear whiter than their surroundings. By analogy with other materials, the upper stress limit to the field of steady-state flow (field 2) is presumably strongly dependent on the applied pressure, but this has not been systematically studied in the current experiments. Because of the large dimensions of our paraffin blocks, high side stresses ($\sigma_3 >$ ca. 1.5 bars) require forces beyond the range of the present machine (cf. Mancktelow 1988). All the experiments reported here were performed with $\sigma_3 = 0.3$ bar, and as discussed below, there are practical problems in using higher confining stresses when studying models formed from components of markedly different strengths.

Above a certain temperature, which approximates the $\alpha-\beta$ phase transition, paraffin wax exhibits a

sudden and very marked weakening (cf. the values at 29.9°C for paraffin wax with melting point 46–48°C and 34.5°C for wax of melting point 50–52°C). This field (field 3) has not been calibrated, as stress levels are so low (<0.2 bar) that they cannot be accurately measured in the present machine. The transition to this field is particularly clear in single-layer folding experiments where there is a sudden and drastic increase in the wavelength of the developed folds as the less-competent matrix wax enters this field.

For a constant confining stress of 0.3 bar, a range of strain rates from 5×10^{-6} to $1 \times 10^{-4} \text{ s}^{-1}$, and a current upper temperature limit for the plane strain machine of 40°C, paraffin waxes of melting point ranges greater than 52°C lie almost entirely within field 1: the field of marked strain softening. These higher melting point waxes are mainly employed in models as more competent components embedded within a weaker matrix. Calibration of such competent waxes at higher confining stress, sufficient to remain within field 2, is inappropriate as these confining stresses could not be maintained during prolonged deformation of the composite models. This follows from the practical limitation that the high confining stresses, many times the flow stress of the weaker matrix, would cause serious extrusion of material from around the model boundaries. More efficient sealing of the model boundaries would involve a penalty in frictional resistance, making accurate measurement of stress-strain curves during the analogue model deformation difficult (Mancktelow 1988).

Discussion and Conclusions

Average geological strain rates are too slow for direct observation and experiments on the development of deformational structures must involve some form of scale model, which is then extrapolated to the natural conditions. If the modelling is restricted to reasonably small-scale structures at low displacement rates, the effects of body forces (gravity and inertial) may be neglected. Strict dynamic similarity

of the surface forces demands, however, that for corresponding particles in the model and in the original, the stress-strain curve must have the same shape and may differ only in the scaling of the stress axis. For heterogeneous deformation, dynamic similarity also requires that the constitutive stress to strain rate relationships of the original and model materials differ only in the proportionality constant. Calibration experiments on paraffin wax demonstrate that, over a limited temperature range, this material can fulfill the requirements for accurate analogue modelling of rocks deforming by power-law creep with a stress exponent in the range of 2 to 4.

Comparison of paraffin and natural rock rheologies
 The available experimental data on natural rocks and minerals indicate that there should be a broad field within the geological range of temperature, strain rate and grainsize in which deformation is accommodated dominantly by intracrystalline dislocation glide and climb with a power-law relationship between strain rate and flow stress (e.g. Frost & Ashby 1982, Ashby & Verrall 1978, White 1976, Schmid 1982). The stress exponent n measured in rocks and single crystals ranges from ca. 1 to 9 (Carter 1976, Tullis 1979, Kirby 1983, Carmichael 1984), with values generally between 2 and 5 for common polycrystalline rocks. The calibrated paraffin waxes, with n values between 2.4 and 4.1, therefore represent excellent analogues for such rocks deforming within the field of power-law creep.

Disadvantages of paraffin as an analogue material

There are some disadvantages of paraffin wax as a modelling material, several of which can be overcome by careful model preparation:

1. Paraffin wax undergoes a marked volume reduction during solidification and cooling. This requires that moulds for models are made oversize and that the blocks are then cut and planed or machined to the correct shape.

2. Paraffin wax layers do not readily stick together, making construction of composite layer models difficult. The most effective method is to maintain composite models at elevated temperature under load, either within the deformation rig itself or in an incubator, for time periods on the order of 12 hours.

3. For the low confining pressures available in the present deformation rig ($\sigma_3 \leq 1.5$ bar), the power-law creep field (field 2) is restricted to quite a narrow homologous temperature range. This is a major

problem with experiments in which a large competency contrast ($> 50:1$) between parts of the model is required, as this requires the use of paraffin waxes with markedly different melting points. For such diverse wax components, the temperature ranges over which deformation occurs by steady-state power-law creep will no longer overlap and experiments in which all components are deforming within this field are not possible.

Advantages of paraffin as an analogue material

The advantages of paraffin wax as a modelling material, in addition to its rheological similarity to common rocks, are:

1. It is cheap, obtainable in large quantities, and available in a range of melting points providing a family of similar materials of differing strengths.
2. It can be easily coloured using standard candle wax dyes, without altering its material properties. This simplifies the construction of composite models.
3. It is easily handled and non-toxic. Very accurate model fabrication is possible by a combination of moulding (from the melt), cutting and planing.
4. It is inherently self-lubricating. When copiously coated with petroleum jelly (vaseline), boundary conditions of very low friction can be achieved in contrast to the serious problems encountered with some other analogue modelling materials (e.g. oil putty, silicone putty, Plasticine, clay).
5. It can be readily reused by melting and remoulding. In this manner, one manufacturer's lot can be used for many experiments, reducing the need for recalibration.

Acknowledgements. Thanks to Ruud Weijermars for his helpful comments on an earlier version of the manuscript and to John-Paul Latham, Martin Casey, Stephan Schmid, John Ramsay, and Jean-Paul Poirier for discussions which helped clarify some of the results presented here.

Appendix

Regression of the raw data is based on the IMSL¹ Library subroutine RLLAV to perform linear regression using the least absolute values criterion. The "% Misfit in Stress" is given by $100^* (\text{Measured Value} - \text{Predicted Value})/\text{Measured Value}$. Strain rates are in terms of natural or logarithmic strain.

¹ IMSL, Inc., 2500 City West Boulevard, Houston, Texas.

Calibration Data for Paraffin Wax of Melting Point 42–44 °C Batch #0

Supplier: Fluka AG, Chemische Fabrik, CH-9470 Buchs, Switzerland

Article Number: 76228

Description: Paraffin wax white congealing point 42–44°

Power-law regression results:

Stress Exponent $n = 4.11$
 Activation Energy $Q = 149 \text{ kcal/mol}$
 Material Constant $A = \exp(248)$

Nr.	Temperature °C	Strain Rate s^{-1}	Stress (bars)	% Misfit in Stress
1	14.5	6.00×10^{-5}	2.18	-2.64
2	14.5	8.00×10^{-5}	2.40	0.00
3	14.7	1.00×10^{-5}	1.35	-2.50
4	14.7	2.30×10^{-5}	1.68	-0.89
5	14.7	4.50×10^{-5}	2.02	1.18
6	14.7	6.00×10^{-5}	2.12	-0.99
7	14.7	1.00×10^{-4}	2.58	6.02
8	14.8	1.70×10^{-5}	1.56	1.26
9	14.8	3.00×10^{-5}	1.83	3.34
10	14.9	1.30×10^{-5}	1.45	2.66
11	18.7	1.00×10^{-5}	0.58	0.00
12	18.7	8.00×10^{-5}	0.90	-6.95
13	18.7	9.00×10^{-5}	0.95	-4.27
14	18.9	7.00×10^{-5}	0.82	-8.87
15	19.1	2.00×10^{-5}	0.58	-8.68
16	19.6	2.00×10^{-5}	0.57	0.61
17	19.6	1.00×10^{-4}	0.88	4.72
18	20.8	1.00×10^{-4}	0.65	0.00
19	20.9	1.00×10^{-4}	0.63	-1.02
20	21.2	1.00×10^{-4}	0.60	0.44
21	21.3	1.00×10^{-4}	0.59	0.86

¹ IMSL Inc., 2500 City West Boulevard, Houston, Texas.

Calibration Data for Paraffin Wax of Melting Point 46–48°C Batch #0

Supplier: E. Merk (Schweiz) AG

Article Number: 7151

Description: Paraffin wax white congealing point 46–48°

Power-law regression results:

Stress Exponent $n = 2.79$
 Activation Energy $Q = 150 \text{ kcal/mol}$
 Material Constant $A = \exp(243)$

Nr.	Temperature °C	Strain Rate s^{-1}	Stress (bars)	% Misfit in Stress
1	17.0	5.02×10^{-6}	5.08	0.00
2	17.0	8.03×10^{-6}	6.05	0.64
3	18.7	5.02×10^{-6}	3.00	1.62
4	18.7	1.01×10^{-5}	3.75	-1.11
5	18.7	2.01×10^{-5}	4.81	-0.88
6	18.7	3.02×10^{-5}	5.50	-2.08
7	20.1	1.01×10^{-5}	2.31	-5.45
8	20.1	5.04×10^{-5}	4.35	0.37
9	22.5	5.00×10^{-5}	2.07	1.27
10	22.5	1.00×10^{-4}	2.62	0.00
11	22.9	1.00×10^{-5}	1.03	1.51
12	22.9	2.00×10^{-5}	1.24	-4.88
13	22.9	4.00×10^{-5}	1.70	1.93
14	22.9	6.00×10^{-5}	1.95	1.13
15	22.9	8.00×10^{-5}	2.10	-1.78
16	22.9	9.00×10^{-5}	2.20	-1.34
17	22.9	1.00×10^{-4}	2.30	-0.67
18	23.1	1.00×10^{-5}	0.95	-0.39
19	23.1	2.00×10^{-5}	1.23	0.60
20	23.1	5.00×10^{-5}	1.73	1.85
21	23.1	3.00×10^{-5}	1.40	-0.99
22	23.1	7.00×10^{-5}	1.97	2.76
23	23.1	1.00×10^{-4}	2.30	5.35
24	24.8	2.00×10^{-5}	0.67	-8.39
25	25.9	1.40×10^{-5}	0.47	2.64
26	25.9	2.00×10^{-5}	0.52	0.00
27	25.9	3.00×10^{-5}	0.63	4.55
28	25.9	5.00×10^{-5}	0.72	-0.30
29	25.9	7.00×10^{-5}	0.83	1.84
30	25.9	9.00×10^{-5}	0.87	-2.47
31	29.9	5.00×10^{-5}	0.11	-98.93 Excluded
32	29.9	1.00×10^{-4}	0.10	-180.54 Excluded

Calibration Data for Paraffin Wax of Melting Point 46–48°C Batch #1

Supplier: E. Merck (Schweiz) AG

Article Number: 7151

Description: Paraffin wax white congealing point 46–48°C

Power-law regression results:

Stress Exponent $n = 2.66$
 Activation Energy $Q = 126 \text{ kcal/mol}$
 Material Constant $A = \exp(204)$

Nr.	Temperature °C	Strain Rate s ⁻¹	Stress (bars)	% Misfit in Stress
1	20.9	1.00×10^{-5}	1.04	0.00
2	20.9	2.00×10^{-5}	1.40	3.59
3	20.9	3.50×10^{-5}	1.60	-4.11
4	20.9	6.00×10^{-5}	2.00	-2.00
5	20.9	1.00×10^{-4}	2.50	1.12
6	25.4	9.83×10^{-6}	0.31	1.75
7	25.4	1.98×10^{-5}	0.38	-4.30
8	25.4	7.84×10^{-5}	0.73	8.91
9	25.4	9.61×10^{-5}	0.77	6.77
10	27.2	1.00×10^{-5}	0.19	0.00
11	27.2	2.00×10^{-5}	0.26	5.16
12	27.2	4.00×10^{-5}	0.32	0.00
13	27.2	6.00×10^{-5}	0.36	-3.53
14	27.2	1.00×10^{-4}	0.44	-2.64

Calibration Data for Paraffin Wax of Melting Point 50–52 °C Batch #0

Supplier: Fluka AG, Chemische Fabrik, CH-9470 Buchs, Switzerland

Article Number: 76229

Description: Paraffin wax white congealing point 50–52°

Power-law regression results:

Stress Exponent $n = 2.42$
 Activation Energy $Q = 127 \text{ kcal/mol}$
 Material Constant $A = \exp(201)$

Nr.	Temperature °C	Strain Rate s^{-1}	Stress (bars)	% Misfit in Stress
1	24.2	4.00×10^{-5}	5.50	0.00
2	24.4	1.00×10^{-5}	2.80	-4.46
3	24.6	2.00×10^{-5}	4.02	8.76
4	26.5	1.00×10^{-5}	1.48	-6.12
5	26.5	5.00×10^{-6}	1.18	0.00
6	26.5	6.00×10^{-5}	3.54	7.10
7	27.8	2.00×10^{-5}	1.30	-9.89
8	27.8	4.00×10^{-5}	1.77	-7.43
9	27.8	8.00×10^{-5}	2.42	-4.58
10	27.8	1.00×10^{-4}	2.65	4.71
11	30.6	1.00×10^{-5}	0.51	6.25
12	30.6	2.00×10^{-5}	0.66	3.58
13	30.6	4.00×10^{-5}	0.95	10.85
14	30.6	8.00×10^{-5}	1.21	6.84
15	30.6	1.00×10^{-4}	1.36	9.12
16	31.5	2.00×10^{-5}	0.48	-2.55
17	31.5	1.01×10^{-4}	0.96	0.00
18	31.5	1.32×10^{-4}	1.02	-5.10
19	31.6	6.00×10^{-5}	0.72	-4.54
20	31.7	1.00×10^{-5}	0.35	0.17
21	31.8	4.00×10^{-5}	0.58	-3.73
22	34.7	4.00×10^{-5}	0.13	-104.72 Excluded
23	34.5	7.00×10^{-5}	0.15	-136.31 Excluded

REFERENCES

- Ashby M.F. & Verrall, R.A. 1978: Micromechanisms of flow and fracture and their relevance to the rheology of the upper mantle. *Phil. Trans. R. Soc. Lond., A* 288, 59–95.
- Barry, B.W. & Grace, A.J. 1971: Rheological properties of white soft paraffin. *Rheol. Acta* 10, 113–120.
- Baumann, M.T. 1986: Verformungsverteilung an Scherzonenden: Analogmodelle und natürliche Beispiele. Doctoral thesis, ETH-Zürich (unpubl.).
- Baumann, M.T. & Mancktelow, N.S. 1987: Initiation and propagation of ductile shear zones (Abstract). *Terra cognita* 7, 47.
- Carmichael, R.S., 1984: *Handbook of Physical Properties*, Vol. 3. CRC Press, Boca Raton, Florida, 340 pp.
- Carter, N.L., 1976: Steady state flow of rocks. *Rev. Geophys. Space Phys.* 14, 301–360.
- Cobbold, P.R., 1975: Fold propagation in single embedded layers. *Tectonophysics* 27, 333–351.
- Dixon, J.M. & Simpson, D.G. 1987: Centrifuge modelling of laccolith intrusion. *J. Struct. Geol.* 9, 87–103.
- Dixon, J.M. & Summers, J.M. 1986: Another word on the rheology of silicone putty: Bingham. *J. Struct. Geol.* 8, 593–595.
- Freund, M., Csikós, R., Keszthelyi, S. & Mózes, G.Y. 1982: *Paraffin Products*. Elsevier, Amsterdam, 335 pp.
- Frost, H.S. & Ashby, M.F., 1982: *Deformation-mechanism Maps*. Pergamon Press, Oxford, 166 pp.
- Hubbert, M.K., 1937: Theory of scale models as applied to the study of geologic structures. *Geol. Soc. Am. Bull.* 48, 1459–1520.
- Kirby, S.M., 1983: Rheology of the lithosphere. *Rev. Geophys. Space Phys.* 21, 1458–1487.
- Kline, S.J., 1965: *Similitude and Approximation Theory*. McGraw-Hill, New York, 229 pp.
- Langhaar, H.L., 1951: *Dimensional Analysis and Theory of Models*. Wiley, New York, 166 pp.
- Latham, J-P. 1979: Experimentally developed folds in a material with a planar mineral fabric. *Tectonophysics* 57, T1–T8.
- Mancktelow, N.S. 1988: An automated machine for pure shear deformation of analogue materials in plane strain. *J. Struct. Geol.* 10, 101–108
- McClay, K.R. 1976: The rheology of plasticine. *Tectonophysics* 33, T7–T15.
- Neurath, C. & Smith, R.B., 1982: The effect of material properties on growth rates of folding and boudinage: experiments with wax models. *J. Struct. Geol.* 4, 215–229.
- Poirier, J.-P., 1985: *Creep of Crystals*. Cambridge University Press, Cambridge, 260 pp.
- Porter, A.W., 1958: *The Method of Dimensions*. Methuen, London, 78 pp.
- Ramberg, H., 1981: *Gravity, Deformation and the Earth's Crust*. Academic Press, London, 452 pp.
- Schmid, S.M., 1982: Laboratory experiments on rheology and deformation mechanisms in calcite rocks and their application to studies in the field. *Mitt. Geol. Inst. ETH-Zürich, Neue Folge Nr. 241*.
- Summers, H.S. 1933: Experimental tectonic geology. *Rept. Aust. & N.Z. Assoc. Advancement Sci.* 21, 49–75.
- Tullis, J.A., 1979: High temperature deformation of rocks and minerals. *Rev. Geophys. Space Phys.* 17, 1137–1154.
- Weijermars, R. 1986: Flow behaviour and physical chemistry of bouncing putties and related polymers in view of tectonic laboratory applications. *Tectonophysics* 124, 325–358.
- Weijermars, R. & Schmeling, H. 1986: Scaling of Newtonian and non-Newtonian fluid dynamics without inertia for quantitative modelling of rock flow due to gravity (including the concept of rheological similarity). *Phys. Earth Planet. Inter.* 43, 316–330.
- White, S. 1976. The effects of strain on the microstructures, fabrics, and deformation mechanisms in quartzite. *Phil. Trans. R. Soc. Lond., A* 283, 69–86.